Nuclear Instruments and Methods in Physics Research A 615 (2010) 182–187

Contents lists available at ScienceDirect

Nuclear Instruments and Methods in Physics Research A

journal homepage: www.elsevier.com/locate/nima

Design and performance of a Compton-coincidence system for measuring non-proportionality of new scintillators

P.B. Ugorowski *, M.J. Harrison, D.S. McGregor

Mechanical and Nuclear Engineering Department, 3002 Rathbone Hall, Kansas State University, Manhattan, KS 66506, USA

ARTICLE INFO

Article history:
Received 18 April 2009
Received in revised form
2 November 2009
Accepted 13 January 2010
Available online 29 January 2010

Keywords:
Non-proportionality
Relative light yield
Compton coincidence
Scintillator

ABSTRACT

A Compton-coincidence scintillator light yield non-proportionality measurement system was constructed and tested. Improved testing procedures and timing resolution have allowed the use of significantly less active excitation sources without lengthening test times or degrading data integrity. Previous methods typically required 100 mCi Cs-137 sources, but an increase in solid angle between source and sample as well as improved timing resolution have allowed the use of sources with activities less than 10 μCi. Representative samples of BGO and NaI(Tl) were tested to validate the system against literature single-source data.

1. Introduction

New scintillator materials must be tested to determine the linearity of the light yield response as a function of the amount of photon energy deposited in the material. Obtaining plots of Relative Light Yield (also called Non-proportionality) vs. Input Photon Energy by direct irradiation using small radioactive sources yields widely-spaced data points, but a Compton-scattering two-detector system can send photons of any desired energy into the crystal being tested, yielding a continuous curve. The linearity of the light yield curve is a limiting factor for the energy resolution of the scintillator material. Early Compton-coincidence systems used a collimated source and a single collimated detector, and relied on measurement of the scattering angle to provide energy information [1–3]. A more recent system eliminates the angle measurement and uses several uncollimated Ge detectors and timing coincidence to determine the energy deposited in the detector being tested [4,5]. The system described herein uses a single Ge detector, completely eliminates collimation and relies on improved coincidence timing to reduce random background counts. What differentiates the system considered here from similar Compton-coincidence systems is the reduced cost, low random background and the ability to use calibration sources of a few μCi for the measurements.

2. Theory

The pulse in a scintillator detector system is formed when an amount of energy is deposited in the scintillating crystal E_e, light is produced with some absolute light yield A, and collected on a photocathode. The photocathode converts the signal to current. The dynodes then amplify the signal before sending it on to the preamplifier, amplifier and Analog-to-Digital Converter (ADC). Overall, from the photocathode through the ADC, the conversion and amplification processes can be combined into a single 'gain' G_S. The resulting pulse height PH_S can be expressed as

$$PH_S = E_e A G_S \tag{1}$$

The absolute light yield is a function of deposited energy. One can define a relative light yield (RLY) as

$$RLY = \frac{A(E_e)}{A(662\ \text{keV})} = \frac{PH(E_e)}{PH(662\ \text{keV}).} \tag{2}$$

In a Compton-scattering event, energy is conserved such that the summation of energy in the scattered photon $E_{\gamma'}$ and the amount of energy deposited E_e, is equal to the original gamma ray energy E_γ.

$$E_\gamma = E_{\gamma'} + E_e. \tag{3}$$

Thus, the relative light yield in the test scintillator crystal can be calculated from the original gamma ray energy (661.657 keV for ^{137}Cs), the pulse height received by the test crystals' ADC and the energy of the gamma photon received by another detector, in this case a large-volume High-Purity Germanium (HPGe) detector. The HPGe detector has 1.1 keV energy resolution (at 122 keV) and is calibrated such that the amplified height of the pulses going to

* Corresponding author. Tel.: +1 785 532 2382 (Office), +1 785 477 2305 (Cell); fax: +1 785 532 7057.
E-mail addresses: pugo@ksu.edu, phil.ugorowski@juno.com (P.B. Ugorowski), mjh7749@yahoo.com (M.J. Harrison), mcgregor@ksu.edu (D.S. McGregor).

0168-9002/$ - see front matter © 2010 Elsevier B.V. All rights reserved.
doi:10.1016/j.nima.2010.01.028

its' ADC represent known energies. Correction must be made for ADC offset, but precise angle information is not needed.

3. Initial system configuration

The initial experimental setup used a collimated 165 mCi ^{137}Cs source. The test crystal was mounted on a Hamamatsu R6231 photomultiplier tube (PMT) as the first detector and a Canberra coaxial GC5020 50% high-purity germanium (HPGe) detector as the second, as shown in Fig. 1.

For each detector, the timing signal passes through an ORTEC 579 Fast Filter Amplifier (FFA), and then on to an ORTEC 583b Constant-Fraction Discriminator (CFD). The CFD combines the input signal with a delayed inverted copy of the input signal to determine when the input signal has reached 20% of full amplitude. This CFD delay is set by adjusting the length of external coils of coaxial cable. The CFD outputs a NIM logic signal when the input pulse reaches 20% of full amplitude. The NIM output signals from both CFDs go to the Universal Logic Module (ULM), made by Cheesecote Mountain CAMAC (CMCAMAC). If the NIM signals arrive at the ULM within a given time difference of each other, called the 'signal width', the ULM generates a delayed NIM gate signal for the ORTEC 413A Analog-to-Digital Converter (ADC) to digitize the pulse heights of the amplified energy signals. The Gate and Delay Generator (GDG) is used to convert the NIM gate signal to the Transistor-Transistor Logic (TTL) gate signal required by the ADC. Timing signals arriving at the ULM with time differences greater than the signal width are deemed to be non-coincident, are not recorded and no system gate is generated. Only the pulse heights of those pairs of energy signals resulting from photons arriving in the two detectors simultaneously are digitized by the ADCs and recorded into the buffer of the CAMAC Crate Controller, also made by CMCAMAC.

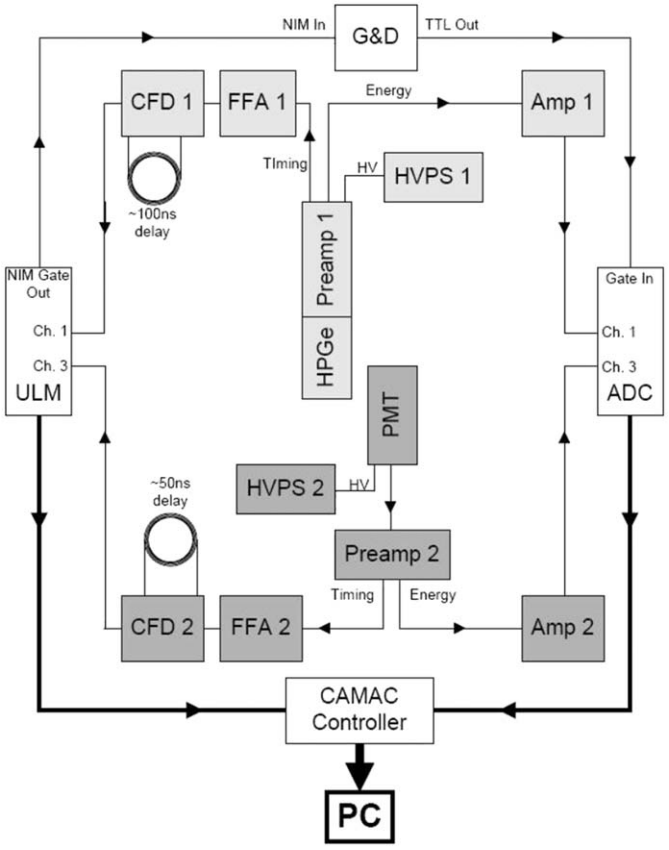

Fig. 1. Block diagram of the coincidence electronics. The modules associated with the Ge detector are shown in light gray, those for the PMT are shown in dark gray.

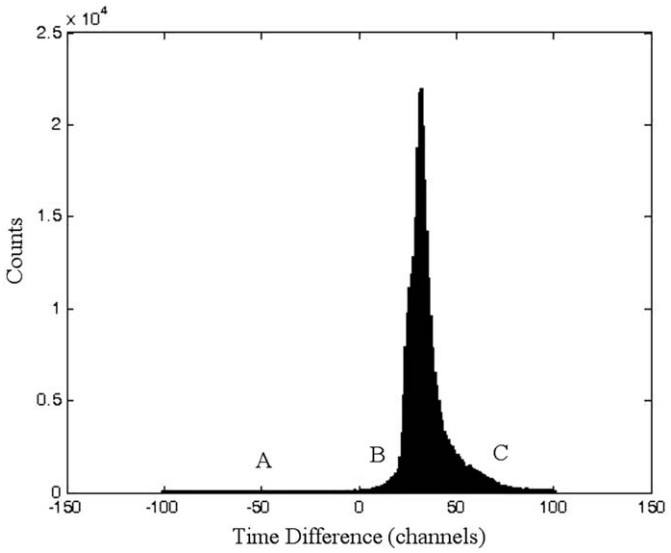

Fig. 2. Histogram of the time differences between BGO scintillator and Ge detector timing signals. The zero channel represents the arrival time of the timing signal from the Ge detector. Each channel number represents 5 ns. In this case, the signal width was set to 1 μs to illustrate the low random background level (region A) far from the coincidence peak. Regions B and C are 'shoulders' arising from timing 'walk' in the Ge detector CFD and the PMT CFD, respectively.

Due to differing signal processing times of the PMT/preamplifier and the Ge detector/preamplifier, the signal width can vary between 100 and 700 ns. The signal width is typically set to be wider than the maximum allowed time difference used in post-processing, so that no coincident events are lost. The minimum time difference between signals arising from coincident photons generally falls within a peak of FWHM 50 ns, the approximate limit of the timing resolution of a large-volume HPGe detector ($\pm$20 ns) plus the timing resolution of the ULM internal clock ($\pm$5 ns). A typical histogram of these recorded time differences, also called a 'coincidence curve', is shown in Fig. 2. The zero channel represents the arrival time of the timing signal from the Ge detector. Each channel represents 5 ns, and the full-width at half-maximum (FWHM) of the peak is 55 ns. Some photons arrive at the two detectors within the signal width time but do not arise from a single Compton-scattering event. Such photons constitute a random background plateau seen far from the peak in Fig. 2. It has been shown [6] that the shoulders of the coincidence curve arise from timing 'walk' in the CFD, and may be included in the analysis.

4. Experimental procedure

The coincidence electronics and high-speed data acquisition system were tested using commercially available NaI(Tl) and BGO crystals, which were cut into pieces measuring 10 mm by 10 mm by 5 mm. The pieces were mounted on the face of the PMT tube using optical grease, covered in Teflon tape and sealed.

Data runs consisted of 20 coincidence runs of one hour each in duration, using the coincidence gating described in the previous section, interspersed with 5–10 min ungated runs of the PMT pulse height spectrum and the Ge detector pulse height spectrum. The purpose of the Ge spectrum was to calibrate the pulse heights of the energy signals coming from the Ge detector with the pulse height corresponding to the 662 keV full-energy peak, to account for gain drift in the Ge detector/preamp between runs. The energy

deposited in the Ge detector is used to calculate the energy deposited in the test scintillator, according to Eq. (3).

The purpose of taking ungated pulse height spectra from the test scintillator was to correct for gain drift during the coincidence run, as well as the drift between runs. The gain drift of the PMT and associated high-voltage power supply using a standard NaI(Tl) sample had a maximum variation of typically $<1.0\%$ during a one-hour run, and that of the HPGe detector was $<0.03\%$. The full-energy peak channel corresponding to 662 keV in the ungated spectra is found by the sorting software before and after a coincidence run. Gain drift during the run was corrected by 'gain scheduling', making a linear fit to the shift in peak position and adjusting the digitized pulse height of each amplified PMT signal during the run by linear interpolation to the fit. The effect of gain scheduling was compared to analysis using only the gains found at the beginning of each one-hour data run. The sorting routines were developed in-house using MATLAB software.

4.1. Post-processing

A 2-D histogram of Relative Light Yield (RLY) values for scattering angles around 0° is shown in Fig. 3. During post-processing, slices of the RLY curve can be assembled into energy bins ranging from 0.5 to 5 keV. For each slice, the data is fitted to a Gaussian curve plus linear background using MATLAB software, as shown in Fig. 4. The mean RLY value for each slice is the mean of the resulting Gaussian for that slice.

The coincidence timing resolution was sufficient to strongly suppress the full-energy peak normally found in scintillator and Ge detector spectra, as this peak cannot result from a Compton-scattering event. Fig. 5 shows the comparison between a spectrum of single events in the NaI(Tl) crystal irradiated with a ^{137}Cs source without coincidence gating, and the events recorded with the same NaI(Tl) crystal with coincidence gating for scattering angles around 0°. Fig. 6 shows a typical spectrum recorded in the Ge detector during coincident events for scattering angles around 0°.

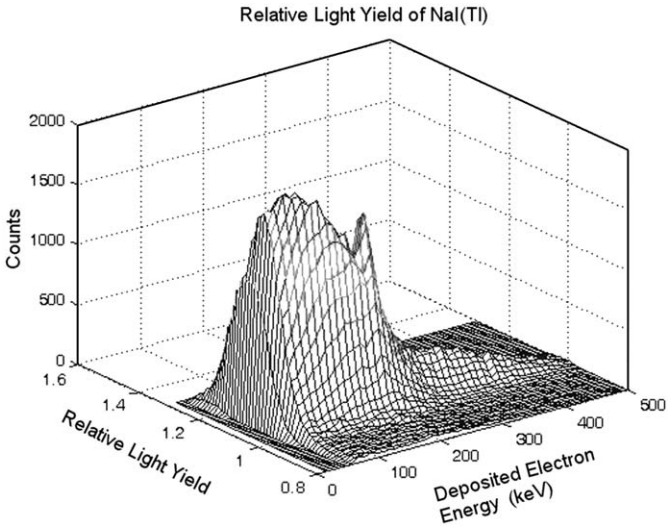

Fig. 3. A mesh plot of RLY values in NaI for scattering angles around 0°. The energy axis corresponds to that portion of the energy of the original photon deposited as Compton-scattered electron energy in the scintillator crystal, as determined by Eq. (3). The backscatter peak, resulting from photons which enter the Ge detector first and scatter back into the scintillator, is visible at values of deposited energy near 180 keV.

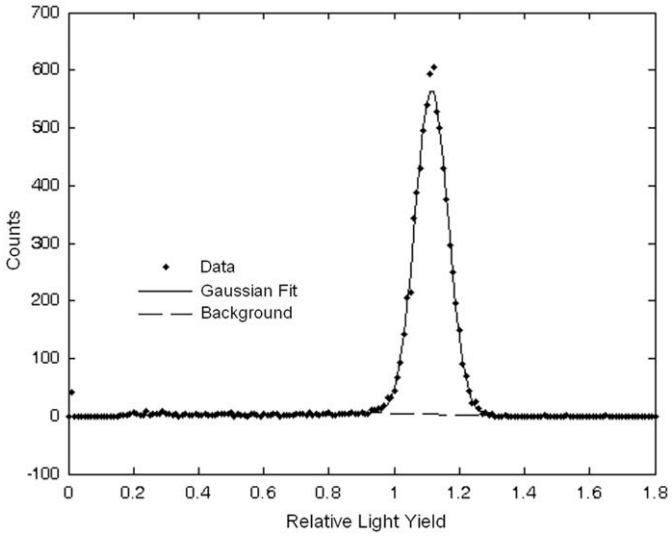

Fig. 4. A representative slice of a RLY curve for NaI(Tl), showing the linear background and the Gaussian fit to the raw data.

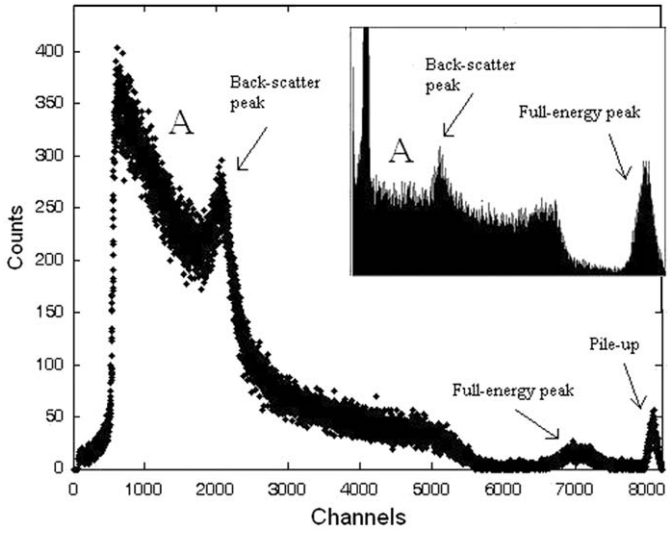

Fig. 5. A spectrum of pulse heights from the NaI scintillator during coincident events, compared with an ungated ^{137}Cs spectrum taken with a NaI scintillator (inset). The region corresponding to deposited electron energies less than 150 keV is marked 'A'. Pile-up can result when more than one photon enters the scintillator during the coincidence time 'window'.

4.2. Alternate configurations

Using the standard setup of a Pb-collimated 165 mCi ^{137}Cs source required source-scintillator distances greater than a few centimeters, particularly at large scattering angles. Scattering from the collimator also increased the background counts, as shown in Figs. 7 and 8. Better results were obtained by using a 9 μCi ^{137}Cs source, eliminating the Pb collimation completely, and moving the Ge detector closer to the PMT (the 'internally-mounted' configuration). The close proximity of the Ge detector to the scintillator in the internally-mounted configuration yields scattering angles from 0° to ±40°, as the Ge detector subtends approximately 80°. Placing the Ge detector as close as possible to the test scintillator and placing the source next to the scintillator

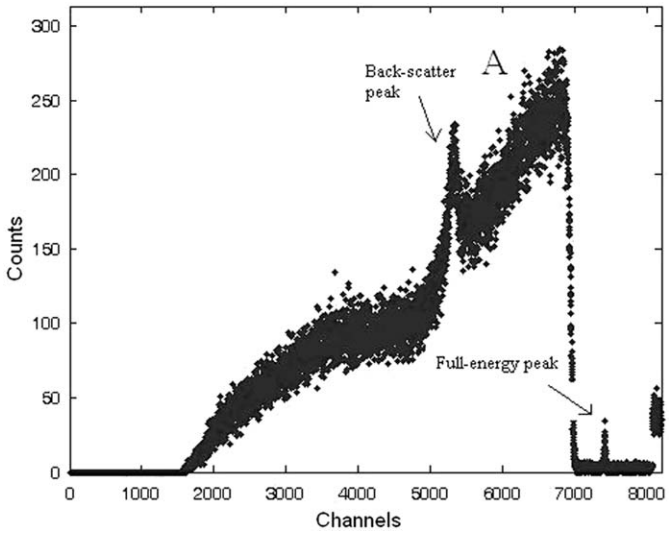

Fig. 6. A pulse height spectrum from the Ge detector during coincident events. The region corresponding to deposited energies in the scintillator of less than 150 keV, according to Eq. (3), is marked 'A'.

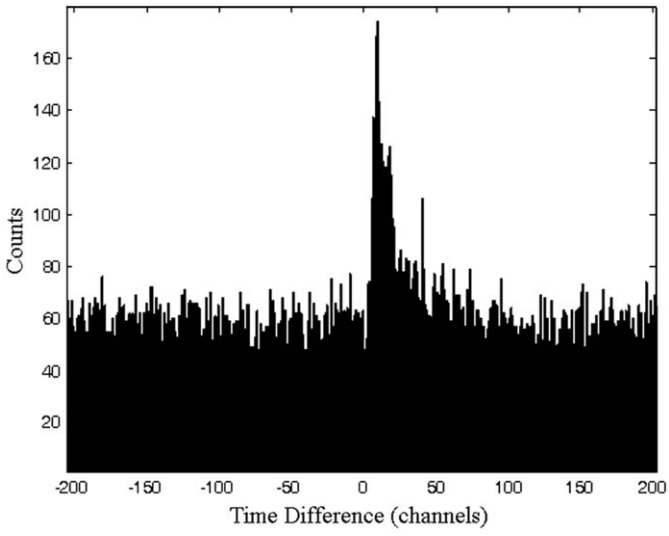

Fig. 7. Histogram of the time differences between NaI scintillator and Ge detector timing signals, as in Fig. 2. This histogram was taken with one hour of data collection at 0º scattering angle, using a 165 mCi source and Pb collimation.

maximizes the range of scattering angles and the count rate. The internally-mounted configuration is shown in Fig. 9, with results shown in Figs. 10 and 11.

For scattering angles around 90°, a rotated scattering geometry (the 'top-mounted' configuration) was used. This configuration yielded RLY results which overlapped the 0° results and extended up to about 500 keV. The top-mounted configuration is shown in Fig. 12, and a mesh plot of the RLY results is shown in Fig. 13.

Overlapping plots of Relative Light Yield vs. deposited gamma energy up to 900 keV of deposited energy were obtained by repeating the top-mounted measurements using ^{54}Mn, with a full-energy peak at 843 keV and ^{65}Zn, with a full-energy peak at 1115 keV. This avoided the issue of low count rates at large scattering angles. These RLY values can be normalized to 662 keV. The unnormalized plots are shown in Figs. 14 and 15.

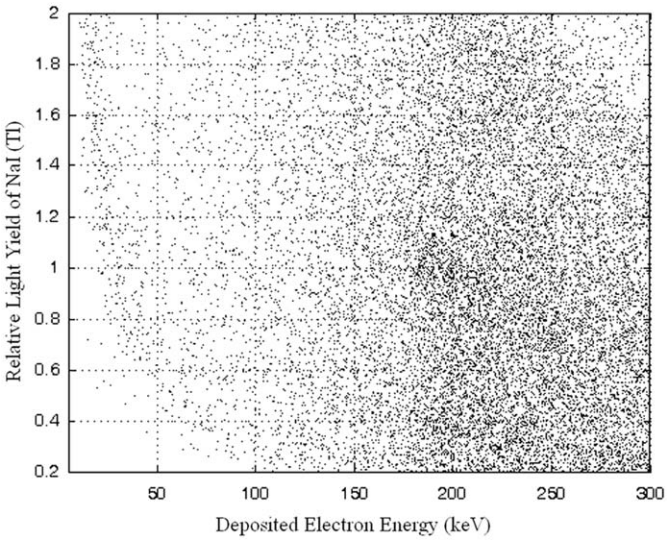

Fig. 8. A scatter plot of RLY vs. deposited electron energy for the same one-hour data run of Fig. 7. This amount of data is insufficient to determine RLY peak values as described in the previous section.

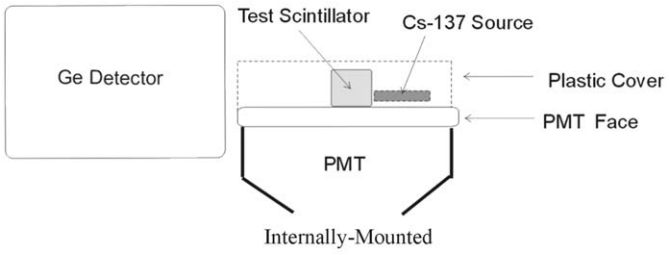

Fig. 9. A configuration for collecting data for scattering angles up to about 40°. The solid angle intercepted by the small scintillator crystal is maximized by placing the ^{137}Cs source as close as possible to the scintillator.

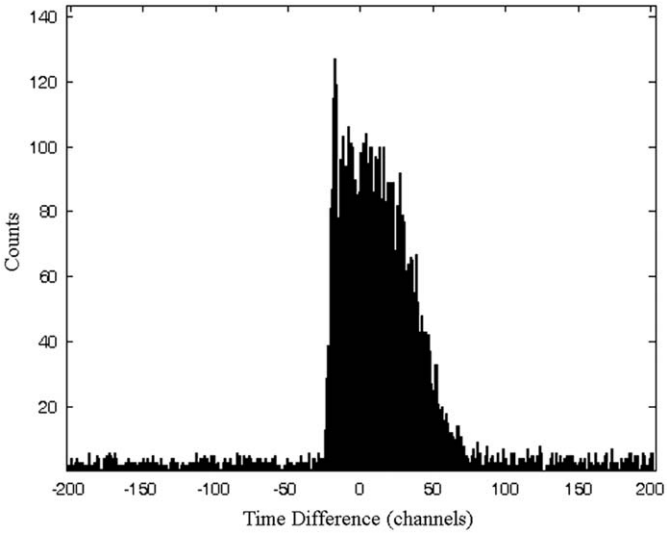

Fig. 10. Histogram of the time differences between NaI scintillator and Ge detector timing signals, taken with one hour of data collection at 0° scattering angle, using a 9μCi source and the internally-mounted configuration of Fig. 9.

5. Results

In comparison with data taken in the standard collimated configuration, the data taken in the internally-mounted and

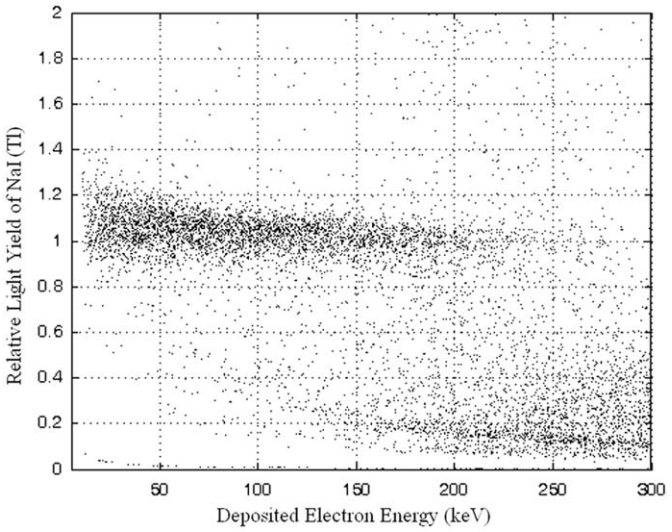

Fig. 11. A scatter plot of RLY vs. deposited electron energy for the same one-hour data run of Fig. 10, using a 9 μCi source and the internally-mounted configuration of Fig. 9. This amount of data begins to show the structure needed to determine RLY peak values, as described in the previous section.

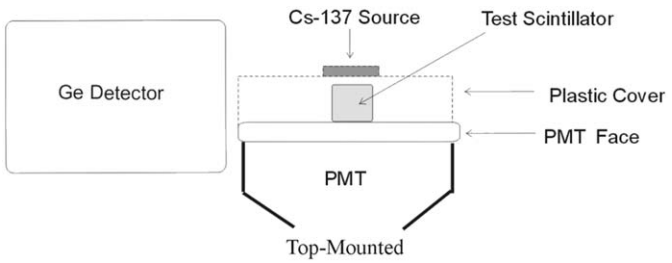

Fig. 12. A configuration for collecting data for scattering angles around 90°.

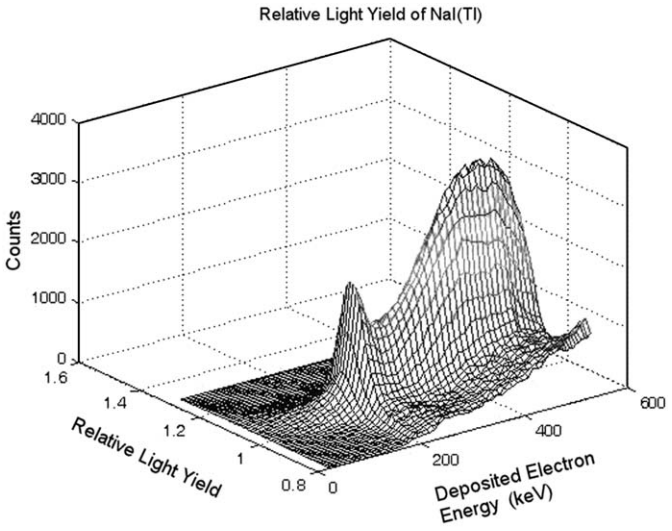

Fig. 13. A mesh plot of RLY values in NaI for scattering angles around 90°, similar to Fig. 3. The backscatter peak, resulting from photons which enter the Ge detector first and scatter back into the scintillator, is visible at values of deposited energy near 180 keV.

top-mounted configurations using sources in the μCi range showed relatively fewer random coincidence counts, and RLY results could be obtained with fewer overall counts. Background

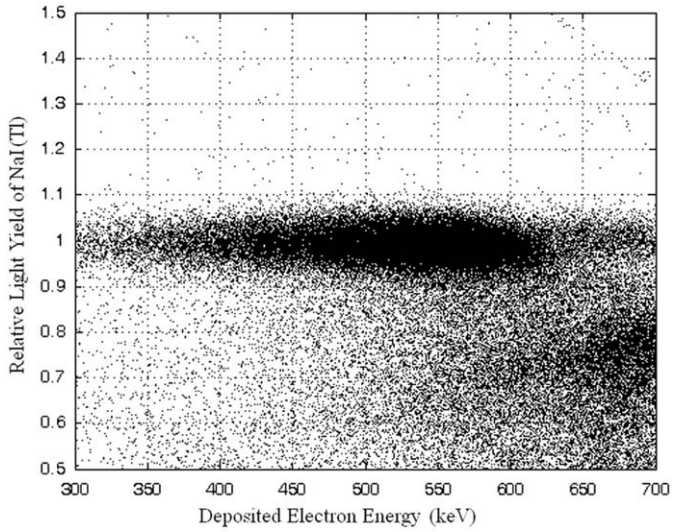

Fig. 14. A scatter plot of RLY vs. deposited electron energy using a ^{54}Mn source and the top-mounted configuration of Fig. 12.

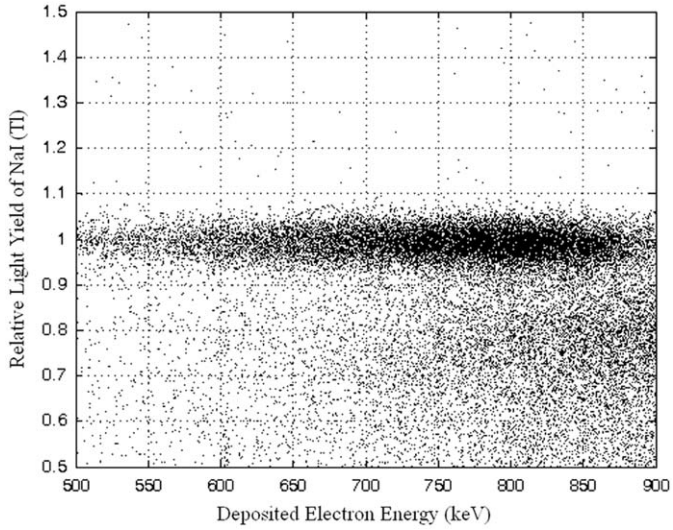

Fig. 15. A scatter plot of RLY vs. deposited electron energy using a ^{65}Zn source and the top-mounted configuration of Fig. 12.

counts arising from non-Compton events were strongly suppressed by the ±25 ns coincidence timing resolution of the system. The effect of gain scheduling was found to be insignificant, allowing for faster post-processing of the data. The most important region of the RLY curve is the region below 150 keV of deposited energy in the scintillator, where deviations from linearity occur for most scintillating materials. The internally-mounted configuration was sufficient for obtaining data in this range without needing to move or rotate either detector. Lower source activity rates yielded cleaner data, as the scintillator was less likely to be still emitting light from a previous event. A comparison of the smoothness of the RLY curves obtained using 9 and 1 μCi sources, with the same approximate number of data events for each, is shown in Fig. 16.

The system runs unattended, and can run overnight or for any length of time. Depending on the size of the test scintillator crystal and the strength of the source, coincidence count rates varied between 35 and 180 cps, although the system was capable of count rates up to 400 cps. A set of 20 consecutive one-hour runs yielded sufficient data to determine the Relative Light Yield

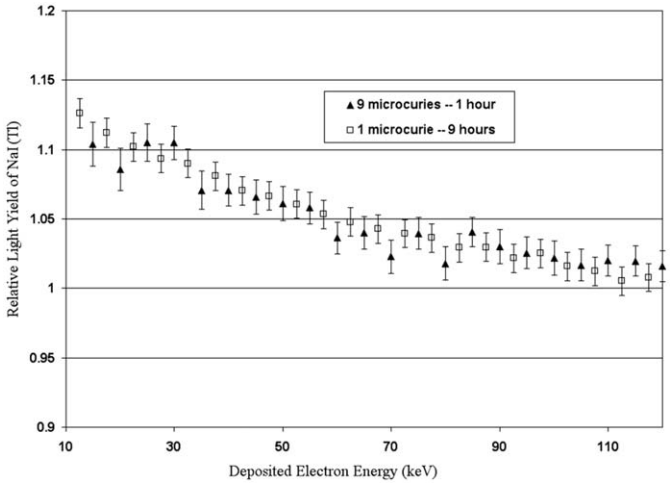

Fig. 16. RLY results for two ^{137}Cs sources, with the same approximate number of data events for each.

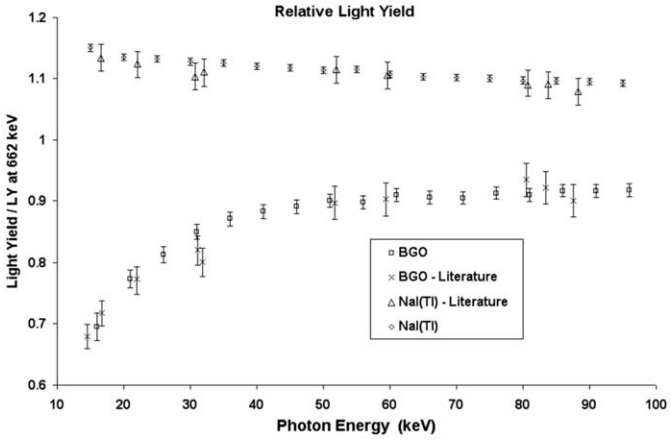

Fig. 17. RLY results for two test crystals, compared to values taken from the literature [7]. Measured RLY values are normalized to literature values near 60 keV.

characteristics of the scintillators tested. These scintillators included commercially available BGO and NaI. Fig. 17 shows results for BGO and NaI.

6. Conclusions

The Compton-coincidence system at Kansas State University S.M.A.R.T. Lab is capable of generating a smooth, continuous plot of Relative Light Yield vs. Input Photon Energy, yielding crucial information about the linearity of the light response of new scintillator materials. The system described here uses a single Ge detector, minimizing setup cost. The timing resolution reduces random coincidence background counts and decreases system dead-time. The percentage of useable data increased when using the alternate configurations, and enabled replacement of large monoenergetic sources in the mCi activity range with 'check' sources in the μCi activity range. Switching to radioactive sources that are reduced in activity by a factor of 10^4 reduces radiation hazards and licensing requirements for anyone wishing to set up such a system for testing scintillating materials.

Acknowledgements

The authors would like to thank Richard Sumner of Cheesecote Mountain CAMAC. This project was funded by the US Department of Energy, NA-22 Advanced Materials and the US Department of Energy, Nuclear Engineering Education Research (NEER) Program.

References

[1] John D. Valentine, Brian D. Rooney, Nucl. Instr. and Meth. A 353 (1994) 37.
[2] Brian D. Rooney, John D. Valentine, IEEE Trans. Nucl. Sci. NS43 (3) (1996) 1271.
[3] W. Mengesha, T.D. Taulbee, B.D. Rooney, J.D. Valentine, IEEE Trans. Nucl. Sci. NS45 (3) (1998) 456.
[4] W.-S. Choong, K.M. Vetter, W.W. Moses, G. Hull, S.A. Payne, N.J. Cherepy, J.D. Valentine, IEEE Trans. Nucl. Sci. NS55 (3) (2008) 1753.
[5] Woon-Seng Choong, Giulia Hull, William W. Moses, Kai M. Vetter, Stephen A. Payne, Nerine J. Cherepy, John D. Valentine, IEEE Trans. Nucl. Sci. NS55 (3) (2008) 1073.
[6] P. Ugorowski, R. Propri, S.A. Karamian, D. Gohlke, J. Lazich, N. Caldwell, R.S. Chakrawarthy, M. Helba, H. Roberts, J.J. Carroll, Nucl. Instr. and Meth. A 565 (2006) 657.
[7] M. Moszynski, in: S. Tavernier et al. (Eds.), Radiation Detectors for Medical Applications, Springer, Dordrecht, 2006, pp. 293–315.